# Cloud-induced stabilization of Greenland surface melt

**Wenshan Wang**[1], **Charles S. Zender**[1,2]

[1]Department of Earth System Science, University of California, Irvine, California, USA
[2]Department of Computer Science, University of California, Irvine, California, USA

**Key Points:**

- Clouds warm Greenland's surface in the accumulation zone on monthly, seasonal, and climatological timescales
- In the ablation zone surface albedo decreases and drives net cloud radiative effects toward cooling, leading to net cloud-induced cooling in the southern ablation zone
- As Greenland warms and darkens, clouds increasingly cool its surface, and reduce energy available for melt

Corresponding author: Wenshan Wang, wenshanw@uci.edu

## Abstract

Net cloud radiative effects (CREs) on Greenland's surface energy budget result from shortwave shading and longwave heating. We use tilt-adjusted automatic weather station data to show that where surface albedo is bright and close to cloud albedo, shading is suppressed and heating dominates. When and where albedo declines (e.g., due to temperature-induced snow metamorphism and/or melt), shading increases more rapidly than cloud greenhouse effects, leading to net cloud-induced cooling. Such cooling is common at lower albedos in the ablation zone, where the 0.57 albedo isopleth distinguishes areas of positive from negative CREs. During extensive surface melt across the Greenland ice sheet (GrIS) in 2012, clouds exerted anomalously strong cooling in the southern ablation zone, and only climatological-mean warming in the accumulation zone. Clouds reduced more than promoted surface melt during summer 2012. These results suggest that clouds will increasingly inhibit surface melt and reduce GrIS dimming in future melt seasons.


## 1 Introduction

Greenland's surface melt has accelerated in the past 30 years [*Tedesco et al.*, 2013; *Velicogna and Wahr*, 2013]. The triggered mass-loss and energy-related feedbacks have great potential to affect global climate in the long-term through, e.g., sea-level rise. Clouds strongly influence surface radiative fluxes in the Arctic due to its persistent cloudiness [*Intrieri et al.*, 2002; *Morrison et al.*, 2011; *Cesana et al.*, 2012; *Shupe et al.*, 2013], dry atmosphere, and highly reflective surface [*Shupe and Intrieri*, 2003]. Clouds may have exerted a profound influence on recent dramatic sea-ice loss and snow melt events [*Kay et al.*, 2008; *Schweiger et al.*, 2008; *Bennartz et al.*, 2013; *Kapsch et al.*, 2015; *Letterly et al.*, 2016; *van Tricht et al.*, 2016]. However, the dearth of coordinated surface-cloud observations in remote and harsh Arctic conditions [*Liu et al.*, 2004; *Shupe et al.*, 2013] has caused cloud radiative effect studies that relate cloud properties directly to the surface energy budget and thus surface melt to be case-dependent and inconclusive on climatological timescales. Recent progress [*Wang et al.*, 2016] in correcting tilt-induced biases in radiometric observations over snow covered surfaces allows us to study cloud effects on GrIS surface processes with unprecedented accuracy on climatological timescales.

Cloud radiative effects (CREs) on the surface energy budget result from a complex interaction between cloud properties (e.g., cloud fraction, cloud water path, and cloud droplet shape and size) and their environment (e.g., surface albedo, moisture profile, solar zenith angle) [*Curry et al.*, 1996; *Shupe and Intrieri*, 2003]. For example, *Kay et al.* [2008] attributes widespread Arctic melting in 2007 to reduced summer cloudiness, which allows more insolation to heat the surface. In contrast, *Bennartz et al.* [2013] argue that warming by shortwave-thin yet longwave-opaque clouds helped to trigger Greenland's widespread surface melt in July, 2012. Given the dynamic nature of snow-covered surfaces, establishing the climatological role of surface CREs on the Greenland Ice Sheet (GrIS) requires *in situ* observations with long coverage and high temporal resolution.

The 30+ automatic weather stations (AWSs) deployed since 1995 on the GrIS provide the best data to study surface CREs there. These AWSs, which measure hourly surface radiation and weather, are arranged from near glacier termini in the ablation zone to Summit atop the GrIS. We use AWS observations [*Wang et al.*, 2016], complemented by clear-sky simulations from a Column Radiation Model (CRM) [*Zender*, 1999], to estimate GrIS CREs from 2008–2013, to assess the leading factors that determine them, and to investigate their influence on the GrIS surface energy budget and thus surface melt. It follows from the definition of CREs and is true worldwide that surface albedo contrast with cloud albedo strongly affects the net result of cloud-induced shortwave (SW) cooling and longwave (LW) warming at the surface. For the GrIS in particular, AWS data show that as albedo decreases due to surplus surface energy, cloud-induced cooling eventually outweighs warming and acts to stabilize the warmest and darkest regions. This process embodies a negative feedback between CREs and surface warming with implications for current and future surface melt on the GrIS.

## 2 Data and Methods

Surface CRE measures the direct radiative effect of clouds on the surface energy budget. Indirect effects of clouds on surface temperature and humidity are not included. Positive CRE indicates that clouds warm the surface, and negative CRE indicates cloud-induced surface cooling. We define AWS CRE as the difference of AWS-measured all-sky radiative fluxes and CRM-simulated clear-sky radiative fluxes at the surface, assuming other meteorological conditions remain constant.

Most AWSs on GrIS are unattended for at least one year at a time, and their data must be interpreted with care. Of the total 25 long-term AWSs we use here, seven are from the Greenland Climate Network (GC-Net), mostly in the accumulation zone (elevation $> 2000\,\mathrm{m}$) [*Steffen et al.*, 1996]. Another 18 stations are from the Programme for Monitoring of the Greenland Ice Sheet (PROMICE), almost all of which are in the ablation zone (elevation $< 2000\,\mathrm{m}$) [*van As and Fausto*, 2011]. The PROMICE stations are usually arranged in pairs, with one station near the equilibrium line and the other well into the ablation zone [*van As and Fausto*, 2011]. Stations from these two networks with less than 10 months of qualified data during the melt seasons from 2008 to 2013 are excluded. The main source of bias in shortwave measurement is station tilt caused by spatially heterogeneous snow melt, snow compaction, and glacier dynamics [*van den Broeke et al.*, 2004; *van As*, 2011; *Stroeve et al.*, 2013; *Wang et al.*, 2016]. *Wang et al.* [2016] further describes our methods and details how we adjust insolation measured by tilted AWSs using the Retrospective, Iterative, Geometry-Based (RIGB) tilt-correction method, to remove per-station mean-absolute biases that average $18\,\mathrm{W\,m^{-2}}$ over the GrIS during melt seasons. "Dome-heating"—absorption of shortwave radiation and heating of pyrgeometer silicon windows—causes the largest biases in AWS-measured longwave surface fluxes [*van den Broeke et al.*, 2004]. It is impossible to estimate this bias accurately without knowing the window temperature. In this study we remove the maximum window heat offset from the longwave AWS measurements—$25\,\mathrm{W\,m^{-2}}$ out of $1000\,\mathrm{W\,m^{-2}}$ of insolation according to the sensor's manual [*Kipp & Zonen*, 2003]— and potentially underestimate CREs.

Clear-sky surface radiative fluxes are simulated every 3 hours using a CRM [*Zender*, 1999] driven by atmospheric profiles from the second version of Modern-Era Retrospective Analysis for Research and Applications (MERRA-2) [*Rienecker et al.*, 2011]. Results were evaluated against high-quality reference radiometric observations from the Atmospheric Radiation Measurement (ARM) site at Barrow, Alaska, U.S.A [*Atmospheric Radiation Measurement (ARM) Climate Research Facility*, 1994]. Throughout the study period, the absolute shortwave simulation discrepancy between ARM measurements and CRM simulations is less than $1\,\mathrm{W\,m^{-2}}$. However, the longwave discrepancy is about $25\,\mathrm{W\,m^{-2}}$, of which $11\,\mathrm{W\,m^{-2}}$ is explained by the 5 K difference in temperature profiles and the $1\,\mathrm{kg\ m^{-2}}$ difference in humidity profiles between MERRA-2 and local radiosonde measurements. To work around the LW simulation bias, we employ the Stefan-Boltzmann equation and use the atmospheric emissivity from the average of all the clear days in one month to estimate the longwave downwelling radiation under clear-sky conditions in that month. This adjustment reduces the mean LW discrepancy to about $5\,\mathrm{W\,m^{-2}}$.

We also use monthly radiative fluxes (to estimate CREs independently of AWSs) and cloud macro-properties from the first and second version of the Modern-Era Retrospective Analysis for Research and Applications (MERRA and MERRA-2) [*Rienecker et al.*, 2011], and the Clouds and the Earth's Radiant Energy System (CERES) [*CERES Science Team*, 2015]. Monthly MERRA-2 radiative fluxes behave well. However, hourly MERRA-2 clear-sky insolation fluxes contain an inexplicable and artificial shift of at least one hour in local solar noon time on 10% of the days during our study period near some AWSs. Hence we rely on monthly rather than hourly data for MERRA-2-estimated CREs.

## 3 Results

We estimate CRE separately for accumulation and ablation-zone stations in the north (N) and south (S) (separated by latitude = 70°N) during the melt season (May–Sept) for 2008–2013 (Fig. 1a). Net CRE remains positive in almost all months in the highly reflective accumulation zone, where the average surface warming by clouds is 21 W m$^{-2}$. CRE becomes negative in a greater number of months in the less reflective ablation zone, especially in the south (-6 W m$^{-2}$) and at low (L) elevations (-12 W m$^{-2}$; Fig. 1b). In the accumulation zone, surface albedo is consistently high (0.81±0.04), from the northern stations to the southern stations. Where high albedo suppresses SW CRE, LW CRE determines net CRE. The decrease of SW CRE drives net CRE changes in the ablation zone with its lower and more variable albedo (0.57±0.19). LW CRE increases from north to south in the ablation zone, probably due to the extra water vapor availability. Lower elevation (L) stations have albedos 0.18 less than their upper (U) elevation counterparts. SW CRE outweighs LW CRE in most months at low (L) stations, and produces net surface cooling. CREs estimated using MERRA (dots) and MERRA-2 (pluses) radiative fluxes generally agree with AWS CREs. CREs from CERES (crosses) are less consistent with the other three, probably due to the coarser CERES spatial resolution that does not resolve areas of heterogeneous albedo (Fig. S1).

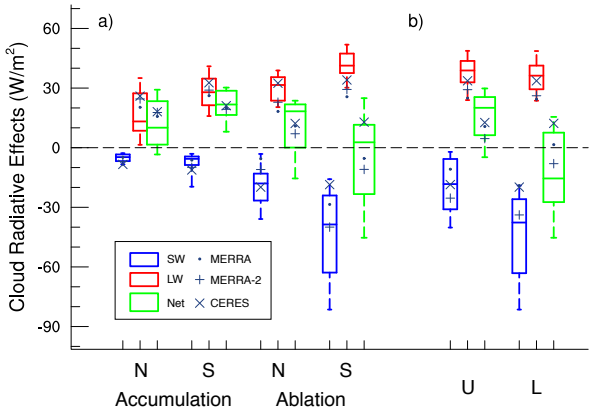


**Figure 1.** Monthly CREs in a) accumulation zones (North and South) and ablation zones (North and South), and b) at upper (U) and lower (L) PROMICE stations. SW, LW and net AWS CREs are represented by blue, red, and green boxes, respectively. Whiskers show min and max, box lines show upper quartile, median, and lower quartile. CREs estimated from MERRA, MERRA-2, and CERES data are overlaid as dots, pluses and crosses, respectively.

AWS CREs generally agree well with MERRA-2 CREs (Fig. 2). Their Root-Mean-Square-Difference (RMSD) is 18 W m$^{-2}$, comparable to the RMSD with MERRA (15 W m$^{-2}$) and CERES (19 W m$^{-2}$; Fig. S1a and c). The albedo = 0.57 isopleth distinctly separates, with 99% accuracy, areas of positive from negative MERRA-2 summertime CREs. Above this threshold, CRE is positive and dominated by LW effects; below the threshold, CRE is negative and dominated by SW effects. The threshold albedo shifts with the availability of insolation from 0.63 in June to 0.50 in August. It drops to 0.25 in September, when clouds begin to exert net surface warming throughout the fall over the entire GrIS (except bare rock). The albedo threshold of 0.57 measured by AWSs also successfully separates stations of positive from negative AWS CRE.

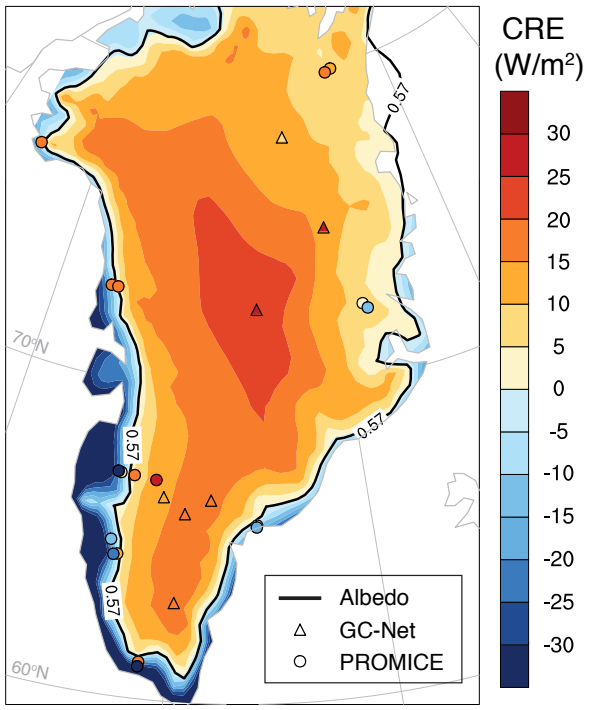


**Figure 2.** AWS CREs (GC-Net in triangles and PROMICE in circles) averaged from May–August, 2008–2013, superimposed on MERRA-2 CREs (color contours). The isopleth where albedo = 0.57 is the solid black line.

Clouds reduce surface insolation and thus SW CREs intensify (become more negative) over lower albedo surfaces where cloud reflectance prevents greater absorption. This effect is most pronounced in the ablation zone. The temporal correlation between monthly surface albedo and MERRA-2 CREs from 2008–2013 is high and significant (Fig. 3a). Monthly AWS CREs in the ablation zone are also significantly ($r = 0.89$, $p < 0.001$) correlated with albedo (Fig. 3b). At high elevations, cloud shielding is limited by the comparable albedos of the surface and clouds. In these areas, cloud temperature, phase, and micro-properties are important to LW CRE and thus net CRE [*Shupe and Intrieri*, 2003]. Nevertheless, cloud fraction, and low-level cloud fraction in particular, is the primary factor controlling CRE temporal and spatial variability. The temporal correlation between low-level cloud fraction and CRE is high and significant throughout the accumulation zone (Fig. 3c). This correlation is also significant ($r = 0.46$, $p = 0.02$) at AWSs (Fig. 3d). Low-level clouds are often present in strong temperature inversions [*Shupe and Intrieri*, 2003], and can efficiently warm the relatively cold surface. The secondary factor controlling GrIS CRE variability in the accumulation zone is condensed water path, especially its liquid component. Clouds containing super-cooled water are ubiquitous and persistent in the Arctic [*Morrison et al.*, 2011; *Cesana et al.*, 2012; *Bennartz et al.*, 2013]. Many small water droplets in mixed-phase Arctic clouds are radiatively more efficient than fewer large ice crystals [*Shupe and Intrieri*, 2003]. The temporal correlation between cloud water path and CREs is significant across a large area and at many stations in the accumulation zone (Fig. S2).

In the ablation zone, albedo change explains most seasonal and inter-annual CRE variability (Fig. 4), with correlation coefficients of 0.90 and 0.96, respectively (Fig. S3). During minimum CRE months (July and August), clouds exert net cooling on the surface. CRE is low-

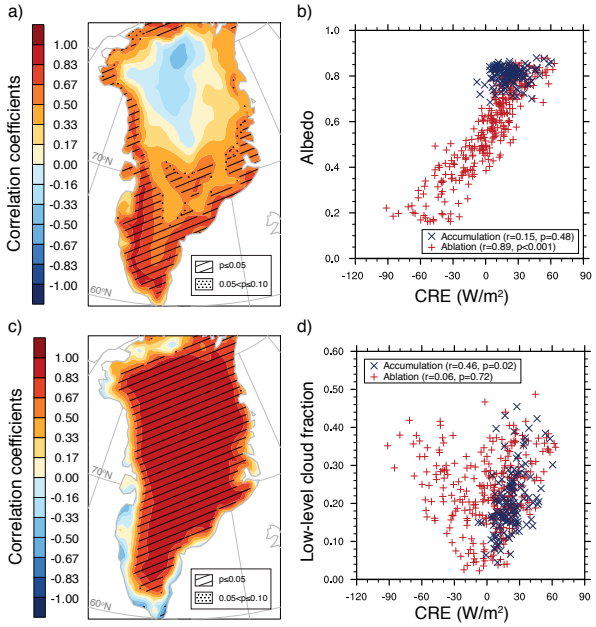


**Figure 3.** Temporal correlation between monthly albedo and CRE in a) MERRA-2 and b) AWS measurements, and correlation between low-level cloud fraction and CRE in c) MERRA-2 and d) AWS measurements. and those significant at the 5% level are shaded by lines in a) and c). In b) and d), CREs in the accumulation and ablation zones are represented by blue crosses and red pluses, respectively.

est in June in the accumulation zone, and increases afterwards until September, likely as a result of changes in both low-level cloud fraction and liquid water path. However, the slightly decreasing inter-annual CRE trend in the accumulation zone is not explicable by concurrent changes in cloud macro-properties (i.e., cloud fraction, water/ice content, height and temperature). Longer observations are needed to confirm the significance of this trend, and reliable measurements of cloud micro-properties may help resolve this enigma. Examination of CREs from AWS and MERRA-2 for 2008–2013 reveals that CREs are unlikely to have significantly contributed to the unparalleled surface melt on GrIS in 2012 [*Nghiem et al.*, 2012]. In the ablation zone, the low summer albedo reduces CREs (Fig. 4b) which becomes negative (net cooling) in the southern ablation zone (Fig. S3). CREs in the accumulation zone in 2012 are close to the long-term mean. Our results do not support *Bennartz et al.* [2013] who argue, based on measurements at Summit, that low-level liquid clouds played a key role in July 2012 Greenland's melt. We found no anomalous cloud-induced heating in the accumulation zone in July, 2012. Moreover, at low elevations more susceptible to surface melt, clouds exerted net cooling.

## 4 Discussion

GrIS surface albedo has been decreasing [*Box et al.*, 2012; *Polashenski et al.*, 2015], and the trend is expected to continue as climate warms and subjects the surface to accelerated metaphorphism [*Flanner and Zender*, 2006]. Our analysis of AWS and reanalysis data shows that this will enhance cloud SW cooling effects and thus diminish net CRE. Moreover, as the liquid water path increases in the warmer and wetter Arctic [*Tedesco et al.*, 2013; *Screen and Simmonds*, 2010], the greenhouse effect of clouds will become saturated while the shading effect of clouds will continue to increase [*Shupe and Intrieri*, 2003]. It is therefore likely that sur-

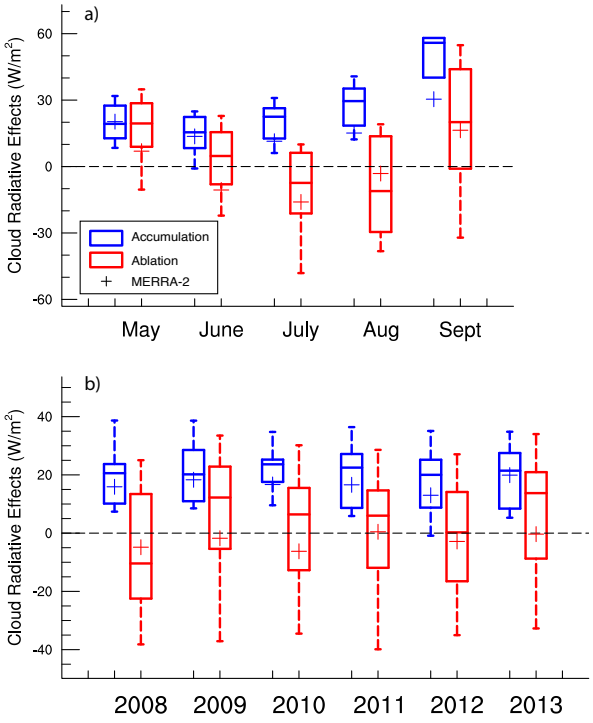


**Figure 4.** Variabilities of CREs in a) seasons and b) long-term in the accumulation zone (blue) and in the ablation zone (red). Box and whiskers show AWS CREs and pluses show MERRA-2 CREs.

face cooling by clouds will outpace cloud-induced surface warming over larger areas and in longer periods on the GrIS. Cloud property-induced variability in CREs is currently small relative to surface albedo-induced variability over the GrIS. So long as this continues, enhanced SW CREs expected in the future will reduce surface energy available for melt and/or metaphorphism, and will act as a negative feedback on surface melt.

## 5 Summary

Surface albedo largely determines the net outcome between cloud-induced surface warming and cooling on the GrIS. Clouds warm the surface by about 21 W m$^{-2}$ in the accumulation zone, and cool the surface by about 12 W m$^{-2}$ in the lower ablation zone. During the 2008–2013 melt seasons, the isopleth of 0.57 albedo separates areas of positive and negative CREs. In the ablation zone, the intensity of the cloud cooling effect is highly positively correlated with albedo: lower albedos associated with warmer environments strengthen cloud-induced surface cooling. The effect of albedo on CRE is suppressed in the accumulation zone where the surface albedo is close to cloud albedo. The seasonal and inter-annual variabilities of CREs in the ablation zone are also highly correlated with albedo: the cooling effect peaks in the lowest albedo months (July and August); the low albedo in 2012 caused by massive surface melt drove net CREs toward cooling. This cooling effect of clouds on the dimming surface acts as a stabilizing mechanism for Greenland's surface melt, and may help to reduce future surface melt.

**Acknowledgments**

The authors acknowledge the GC-Net and PROMICE teams for providing AWS measurements. CERES data were obtained from the NASA Langley Research Center Atmospheric Science Data Center; MERRA and MERRA-2 data were obtained from the Global Modeling and Assimilation Office and the Goddard Earth Sciences Data and Information Services Center. Supported by NASA ACCESS NNX14AH55A and by DOE ACME DE-SC0012998.

## References

Atmospheric Radiation Measurement (ARM) Climate Research Facility (1994), *Data Quality Assessment for ARM Radiation Data (QCRAD1LONG). 2008-05-01 to 2013-05-31, 71.323 N 156.609 W: North Slope Alaska (NSA) Central Facility, Barrow AK (C1).*, Oak Ridge, Tennessee, USA, doi:10.5439/1027372.

Bennartz, R., M. D. Shupe, D. D. Turner, V. P. Walden, K. Steffen, C. J. Cox, M. S. Kulie, N. B. Miller, and C. Pettersen (2013), July 2012 Greenland melt extent enhanced by low-level liquid clouds, *Nature*, *496*(7443), 83–86, doi:10.1038/nature12002.

Box, J. E., X. Fettweis, J. C. Stroeve, M. Tedesco, D. K. Hall, and K. Steffen (2012), Greenland ice sheet albedo feedback: thermodynamics and atmospheric drivers, *The Cryosphere*, *6*(4), 821–839, doi:10.5194/tc-6-821-2012.

CERES Science Team (2015), *NASA Atmospheric Science Data Center (ASDC)*, Hampton, VA.

Cesana, G., J. E. Kay, H. Chepfer, J. M. English, and G. de Boer (2012), Ubiquitous low-level liquid-containing Arctic clouds: New observations and climate model constraints from CALIPSO-GOCCP, *Geophysical Research Letters*, *39*(20), L20,804, doi:10.1029/2012GL053385.

Curry, J. A., W. B. Rossow, D. Randall, and J. L. Schramm (1996), Overview of Arctic Cloud and Radiation Characteristics, *Journal of Climate*, *9*, 1731–1764, doi:10.1175/1520-0442(1996)009¡1731:OOACAR¿2.0.CO;2.

Flanner, M. G., and C. S. Zender (2006), Linking snowpack microphysics and albedo evolution, *Journal of Geophysical Research*, *111*(D12), D12,208, doi:10.1029/2005JD006834.

Intrieri, J. M., M. D. Shupe, T. Uttal, and B. J. McCarty (2002), An annual cycle of Arctic cloud characteristics observed by radar and lidar at SHEBA, *Journal of Geophysical Research*, *107*(C10), 8030, doi:10.1029/2000JC000423.

Kapsch, M.-L., R. G. Graversen, M. Tjernström, R. Bintanja, M.-L. Kapsch, R. G. Graversen, M. Tjernström, and R. Bintanja (2015), The Effect of Downwelling Longwave and Shortwave Radiation on Arctic Summer Sea Ice, *Journal of Climate*, *29*, 1143–1159, doi:10.1175/JCLI-D-15-0238.1.

Kay, J. E., T. L'Ecuyer, A. Gettelman, G. Stephens, and C. O'Dell (2008), The contribution of cloud and radiation anomalies to the 2007 Arctic sea ice extent minimum, *Geophysical Research Letters*, *35*(8), L08,503, doi:10.1029/2008GL033451.

Kipp & Zonen (2003), Instruction manual for Kipp & Zonen CG 3 pyrgeometer.

Letterly, A., J. Key, and Y. Liu (2016), The influence of winter cloud on summer sea ice in the Arctic, 1983-2013, *Journal of Geophysical Research: Atmospheres*, *121*(5), 2178–2187, doi:10.1002/2015JD024316.

Liu, Y., J. R. Key, R. a. Frey, S. a. Ackerman, and W. Menzel (2004), Nighttime polar cloud detection with MODIS, *Remote Sensing of Environment*, *92*(2), 181–194, doi:10.1016/j.rse.2004.06.004.

Morrison, H., G. de Boer, G. Feingold, J. Harrington, M. D. Shupe, and K. Sulia (2011), Resilience of persistent Arctic mixed-phase clouds, *Nature Geoscience*, *5*(1), 11–17, doi:10.1038/ngeo1332.

Nghiem, S. V., D. K. Hall, T. L. Mote, M. Tedesco, M. R. Albert, K. Keegan, C. A. Shuman, N. E. DiGirolamo, and G. Neumann (2012), The extreme melt across the Greenland ice sheet in 2012, *Geophysical Research Letters*, *39*(20), L20,502, doi:

10.1029/2012GL053611.

Polashenski, C. M., J. E. Dibb, M. G. Flanner, J. Y. Chen, Z. R. Courville, A. M. Lai, J. J. Schauer, M. M. Shafer, and M. Bergin (2015), Neither dust nor black carbon causing apparent albedo decline in Greenland's dry snow zone: Implications for MODIS C5 surface reflectance, *Geophysical Research Letters*, *42*(21), 9319–9327, doi:10.1002/2015GL065912.

Rienecker, M. M., M. J. Suarez, R. Gelaro, R. Todling, J. Bacmeister, E. Liu, M. G. Bosilovich, S. D. Schubert, L. Takacs, G.-K. Kim, S. Bloom, J. Chen, D. Collins, A. Conaty, A. da Silva, W. Gu, J. Joiner, R. D. Koster, R. Lucchesi, A. Molod, T. Owens, S. Pawson, P. Pegion, C. R. Redder, R. Reichle, F. R. Robertson, A. G. Ruddick, M. Sienkiewicz, and J. Woollen (2011), MERRA: NASA's Modern-Era Retrospective Analysis for Research and Applications, *Journal of Climate*, *24*(14), 3624–3648, doi:10.1175/JCLI-D-11-00015.1.

Schweiger, a. J., J. Zhang, R. W. Lindsay, and M. Steele (2008), Did unusually sunny skies help drive the record sea ice minimum of 2007?, *Geophysical Research Letters*, *35*(10), L10,503, doi:10.1029/2008GL033463.

Screen, J. A., and I. Simmonds (2010), The central role of diminishing sea ice in recent Arctic temperature amplification, *Nature*, *464*(7293), 1334–1337, doi:10.1038/nature09051.

Shupe, M. D., and J. M. Intrieri (2003), Cloud Radiative Forcing of the Arctic Surface : The Influence of Cloud Properties, Surface Albedo, and Solar Zenith Angle, *Journal of Climate*, *17*, 616–628, doi:10.1175/1520-0442(2004)017¡0616:CRFOTA¿2.0.CO;2.

Shupe, M. D., D. D. Turner, V. P. Walden, R. Bennartz, M. P. Cadeddu, B. B. Castellani, C. J. Cox, D. R. Hudak, M. S. Kulie, N. B. Miller, R. R. Neely, W. D. Neff, and P. M. Rowe (2013), High and Dry: New Observations of Tropospheric and Cloud Properties above the Greenland Ice Sheet, *Bulletin of the American Meteorological Society*, *94*(2), 169–186, doi:10.1175/BAMS-D-11-00249.1.

Steffen, C., J. Box, and W. Abdalati (1996), Greenland Climate Network: GC-Net, *US Army Cold Regions Reattach and Engineering (CRREL), CRREL Special Report*, pp. 98–103.

Stroeve, J., J. E. Box, Z. Wang, C. Schaaf, and A. Barrett (2013), Re-evaluation of MODIS MCD43 Greenland albedo accuracy and trends, *Remote Sensing of Environment*, *138*, 199–214, doi:10.1016/j.rse.2013.07.023.

Tedesco, M., X. Fettweis, T. Mote, J. Wahr, P. Alexander, J. E. Box, and B. Wouters (2013), Evidence and analysis of 2012 Greenland records from spaceborne observations, a regional climate model and reanalysis data, *The Cryosphere*, *7*(2), 615–630, doi:10.5194/tc-7-615-2013.

van As, D. (2011), Warming, glacier melt and surface energy budget from weather station observations in the Melville Bay region of northwest Greenland, *Journal of Glaciology*, *57*(202), 208–220, doi:10.3189/002214311796405898.

van As, D., and R. S. Fausto (2011), Programme for Monitoring of the Greenland Ice Sheet ( PROMICE ): first temperature and ablation records, *Geological Survey of Denmark and Greenland Bulletin*, *23*, 73–76.

van den Broeke, M., D. van As, C. Reijmer, and R. van de Wal (2004), Assessing and Improving the Quality of Unattended Radiation Observations in Antarctica, *Journal of Atmospheric and Oceanic Technology*, *21*(9), 1417–1431, doi:10.1175/1520-0426(2004)021¡1417:AAITQO¿2.0.CO;2.

van Tricht, K., S. Lhermitte, J. T. M. Lenaerts, I. V. Gorodetskaya, T. S. L'Ecuyer, B. Noël, M. R. van den Broeke, D. D. Turner, and N. P. M. van Lipzig (2016), Clouds enhance Greenland ice sheet meltwater runoff, *Nature Communications*, *7*, 10,266, doi:10.1038/ncomms10266.

Velicogna, I., and J. Wahr (2013), Time-variable gravity observations of ice sheet mass balance: Precision and limitations of the GRACE satellite data, *Geophysical Research Letters*, *40*(12), 3055–3063, doi:10.1002/grl.50527.

Wang, W., C. S. Zender, D. vanAs, P. C. J. P. Smeets, and M. R. vandenBroeke (2016), A Retrospective, Iterative, Geometry-Based (RIGB) tilt-correction method for radiation observed by automatic weather stations on snow-covered surfaces: application to Greenland, *The Cryosphere*, *10*(2), 727–741, doi:10.5194/tc-10-727-2016.

Zender, C. S. (1999), Global climatology of abundance and solar absorption of oxygen collision complexes, *Journal of Geophysical Research*, *104*(D20), 24,471, doi:10.1029/1999JD900797.